Available online at https://ifejost.oauife.edu.ng

IFE JOURNAL OF SCIENCE AND TECHNOLOGY

Vol 7. No. 1 (2023) 160–176

Comparative study of the photovoltaic properties of corrole- and phthalocyanine-based sensitizers for dye-sensitized solar cell (DSSC) application: a theoretical investigation

K. Sanusi[1,*], N. O. Fatomi[1], and P. B. Khoza[2]

[1]Department of Chemistry, Obafemi Awolowo University, Ile-Ife, Nigeria

[2]School of Chemistry and Physics, University of Kwazulu Natal, Westville Campus, Durban, 3629, South Africa

*Corresponding author: sosanusi@oauife.edu.ng

Telephone: +234-803-756-8619, +234-705-560-2893

Abstract

In this paper, the photovoltaic efficiencies obtained via the electronic property study of corroles and phthalocyanines (Pcs) with metal and hydrogen atom centers by means of density functional theory (DFT, using hybrid functionals) are presented. The investigation aimed at showing the possible advantages of coordinated metal corroles over that of phthalocyanines as redox active complexes for dye-sensitized solar cell (DSSC) application. This was with a view to finding a solution to the Nigerian electricity crisis. The energy gap (δ_p) between the lowest unoccupied molecular orbital (LUMO) and TiO_2 conduction band (CB), and their relative positions to each other revealed that most of the complexes are essentially not suitable for DSSC application. The computed δ_p values for the corroles (-12.4 – 7.10 eV) and the Pcs (-5.71 – 7.92 eV) were found to be significantly higher than the recommended value (~0.40 eV), except for molecule C10 (0.9 eV) whose value appears to be the closest to 0.4 eV. It was also observed that a considerable number of the dye LUMOs showed non-alignment to the TiO_2 CB edge. Based on this finding, we conclude that most of the studied complexes are structurally deficient to meet the minimum specifications to be applicable as DSSC sensitizers. However, some of the corrole (C10) and Pc (P3 and P4) molecules produced a considerably high IPCE values (in the order of 10^{12}). The photovoltaic performance of these set of molecules could be further improved through structural modification and extension of their π-conjugation.

Keywords**:** *Electrochemical potential, electron injection, electron recombination, Nigeria*

Introduction

According to the data obtained from World Bank, only 55.4% of Nigerians have access to electricity as at 2019 (The World Bank Group, 2021, para 1). In the coming years, the world may face a major challenge of global rise in energy demand as the latest release of

International Energy Outlook 2017 of U.S., Energy Information Administration, has projected that the world energy consumption will increase by 28% between 2015 and 2040 (The International Energy Agency, 2017, para 5). This implies that Nigeria, as well as other developing countries, will need to find sustainable and affordable ways to meet their growing energy needs to improve their living standards. The rapid depletion of fossil fuel reserves as well as dreadful environmental impacts that accompany their combustion has demanded for the provision of clean and renewable energy sources (Carella *et al*., 2018).

One of the promising alternatives is the use of dye-sensitized solar cells (DSSCs), which are low-cost, easy-to-fabricate, and environmentally friendly devices that can convert solar energy into electricity (Carella *et al*., 2018). The theoretically predicted efficiency of DSSCs was approximately 20% (Snaith, 2010; Frank *et al*., 2004), however, several reports have shown that higher efficiency can be achieved by fine-tuning the properties of the components of the DSSC (Carella *et al*., 2018). In DSSCs, the efficiency of one component is dependent on the performance of another, hence, the development of only one component is not always sufficient to improve the overall efficiency of the entire DSSC (Raffaelle, 2006). Also notably, the overall DSSC performance can be limited by the electron transport in the nanocrystal boundaries of dye/TiO_2 nanoparticles, and the electron recombination with the oxidized dye molecule during the electron injection process (Andrews *et al*., 2004). As such, DSSC performance depends largely on the choice of the dye.

The use of corrole- and phthalocyanine-based dyes have attracted considerable attention due to their excellent optical and electronic properties (Aviv-Harel and Gross, 2009; Urbani *et al*., 2019). They are both analogues of porphyrin, which has demonstrated a remarkably high PCE value ~13% and above as a photosensitizer for DSSC (Mathew *et al*., 2014). However, despite their structural similarity, coordinated metal corroles often show higher and variable oxidation states than the corresponding metal phthalocyanine complexes (Pierloot *et al*., 2010). This is an interesting feature for photoelectrochemical processes involved in the operations of DSSCs. In addition, corroles have recently been shown to possess remarkable thermal stability to a temperature as high as 200°C (Sudhakar *et al*., 2015). These distinctive properties put corroles as a valuable organic material for application as photosensitizers in DSSCs. The maximum power conversion efficiency (PCE) that has been reported for a corrole-based DSSC is 4.2% (Higashino *et al*., 2020), a rather too low efficiency value relative to that of porphyrin (Mathew *et al*., 2014).

Pc-based DSSCs have shown marked increase in efficiency over the years, resulting in an approximate PCE of 6% (Urbani *et al*., 2019). They have distinct absorption properties with two prominent bands, B- and Q-bands, in the UV-Vis and the near-IR regions, respectively (Gorduk, 2019; Gorduk and Altindal, 2019). This unique absorption patterns of Pcs make them highly suitable for DSSC application (Hamann *et al*., 2008). This study, therefore, investigates the performance of ten corroles (Figure 1) and nine Pcs (Figure 2) as potential sensitizers for DSSC application.

The selected metals, Mn, Zn, Fe, Cu and Ni have been widely employed by other

researchers before (Tunç *et al*., 2019; Karaca *et al*., 2018; Ali *et al*., 2016; Aviv and Gross, 2007; Brennan *et al*., 2015; Sanusi *et al*., 2020; Polat *et al*., 2018; Srikanth *et al*., 2015; Zhu and Liang, 2015). However, in this study, they were chosen to bring into play their role as redox active agents, with the hope of improving the electron transfer property of the metal-organic complexes, an important property for efficient electron transport in DSSC operation.

A

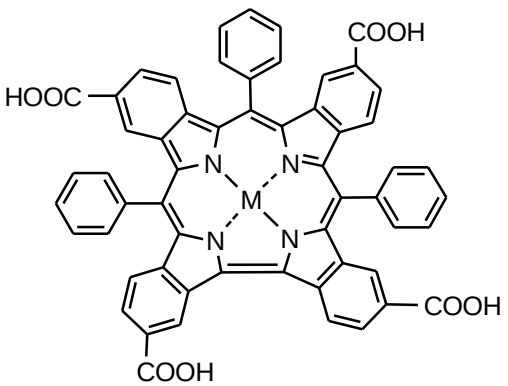

C1: M = Mn, **C2:** M = Zn, **C3:** M = Cu, **C4:** M = Fe, **C5:** M = H_3

B

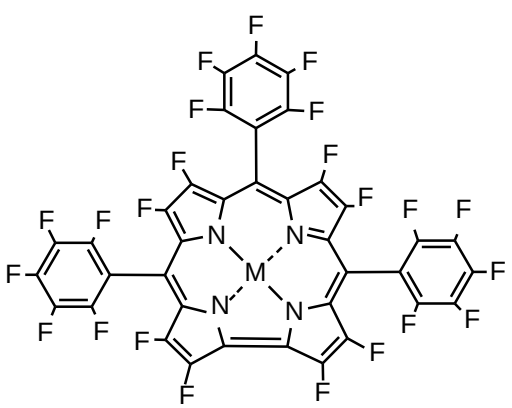

C6: M = Zn, **C7:** M = Mn, **C8:** M = Cu, **C9:** M = Fe, **C10:** M = H_3

Figure 1: Molecular structures of the investigated corroles, (A) *meso*-tris(phenyl)-α-tetra-carboxybenzocorrole, (B) *meso*-tris(pentafluorobenzo)octafluorocorrole.

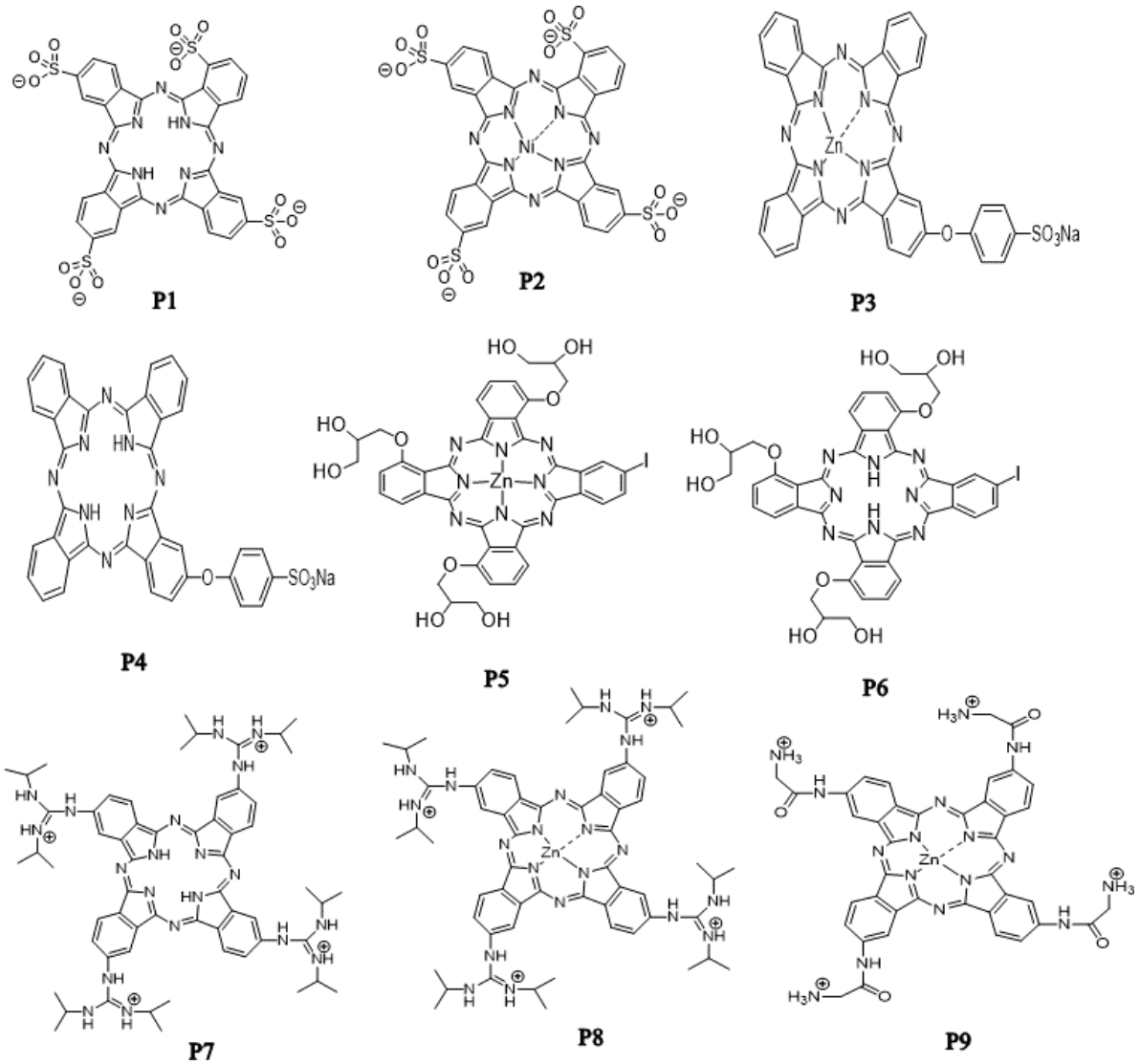

Figure 2: Molecular structures of the investigated α- (**P1**-**P4**, **P7**-**P9**) and β- (**P5** & **P6**) substituted phthalocyanines Density Functional Theory (DFT) geometry optimizations were performed with Gaussian.

Computational Details

16 program suite (Gaussian 16, Revision C.01, 2016), using 6-31g(d) basis set for molecules containing only hydrogen and non-metal atoms. Convergent calculations were

obtained for corroles with non-zero overall charges ($q \neq 0$) after adding a diffused function to 6-31g(d) basis set (Table 1). Similarly for the Pcs, a diffused and *p* polarization functions were added to 6-31g(d) to obtain convergent calculations for molecules with $q \neq 0$ (Table 1). Effective core potentials (ECPs), LANL2DZ, were incorporated into the basis set for both corrole and phthalocyanine metal complexes. For all the macrocycles, the optimized geometry was found and confirmed by frequency analyses to correspond to the minimum energy on the potential energy surface (PES). Vibrational and time-dependent (TD) electronic DFT calculations were carried out using the same basis set described above for each category of the macrocycles. The TDDFT calculations were performed for $N = 60$ electronic states. All calculations were performed in vacuum using the hybrid B3LYP functional (Lee *et al*., 1988; Becke, 1992a; 1992b; Becke, 1993). The results of the electronic calculations were analyzed and used to estimate the potential energy gap (δ_p) and the incident photon conversion efficiencies (IPCEs) of the macrocycles to predict their photovoltaic performance in accordance with literature procedure (Sanusi *et al*., 2019; Sanusi *et al*., 2020; Sanusi *et al*., 2023).

Table 1: Basis Sets Used for Optimization and Frequency Calculations, and the Overall Charges of the Studied Molecules.

Molecule	Geometry Optimization	Vibrational Frequency	Net charge
C1	6-31+g(d)/LANL2DZ	6-31+g(d)/LANL2DZ	+4
C2	6-31+g(d)/LANL2DZ	6-31+g(d)/LANL2DZ	-1
C3	6-31+g(d)/LANL2DZ	6-31+g(d)/LANL2DZ	-2
C4	6-31+g(d)/LANL2DZ	6-31+g(d)/LANL2DZ	-1
C5	6-31g(d)	6-31g(d)	0
C6	6-31+g(d)/LANL2DZ	6-31+g(d)/LANL2DZ	-1
C7	6-31+g(d)/LANL2DZ	6-31+g(d)/LANL2DZ	+4
C8	6-31+g(d)/LANL2DZ	6-31+g(d)/LANL2DZ	-2

C9	6-31g(d)+/LANL2DZ	6-31+g(d)/LANL2DZ	-1
C10	6-31g(d)	6-31g(d)	0
P1	6-31+g(d,p)/LANL2DZ	6-31+g(d,p)/LANL2DZ	-4
P2	6-31+g(d,p)/LANL2DZ	6-31+g(d,p)/LANL2DZ	-4
P3	6-31g(d)/LANL2DZ	6-31g(d)/LANL2DZ	0
P4	6-31g(d)/LANL2DZ	6-31g(d)/LANL2DZ	0
P5	6-31g(d)/LANL2DZ	6-31g(d)/LANL2DZ	0
P6	6-31g(d)/LANL2DZ	6-31g(d)/LANL2DZ	0
P7	6-31+g(d,p)/LANL2DZ	6-31+g(d,p)/LANL2DZ	+4
P8	6-31+g(d,p)/LANL2DZ	6-31+g(d,p)/LANL2DZ	+4
P9	6-31+g(d,p)/LANL2DZ	6-31+g(d,p)/LANL2DZ	+4

Results and Discussions

Electronic Property

Figures 3 and 4 are the computed electronic absorption and emission spectra of the investigated corroles and phthalocyanines, respectively. The absorption bands were expressed as vertical excitation peaks. The spectroscopic properties of the studied corroles and Pcs are similar to those obtained experimentally. For instance, the UV-Vis spectrum of compound C6 showed an intense Soret band around 414 nm and a weaker Q-band around 550 nm, which is similar to the experimentally obtained UV-Vis spectrum for tetrabenzocorroles (Pomarico *et al*., 2013; Pomarico *et al*., 2011). This similarity was also observed between the experimentally and theoretically obtained spectroscopic properties of the studied phthalocyanines. For instance, P3 has a broad B band around 340 nm and an intense Q band between 620 nm range which is a familiar spectral property of a typical phthalocyanine (Gorduk, 2019; Gorduk and Altindal, 2019). The emission spectra exhibit the expected emission redshift relative to the corresponding absorption spectra (Lakowicz, 2006; Noomnarm and Clegg 2009). The absorption and emission energies of the studied dyes fall within the spectral range of 350 – 800 nm, as required for DSSC application

(Carella *et al*., 2018).

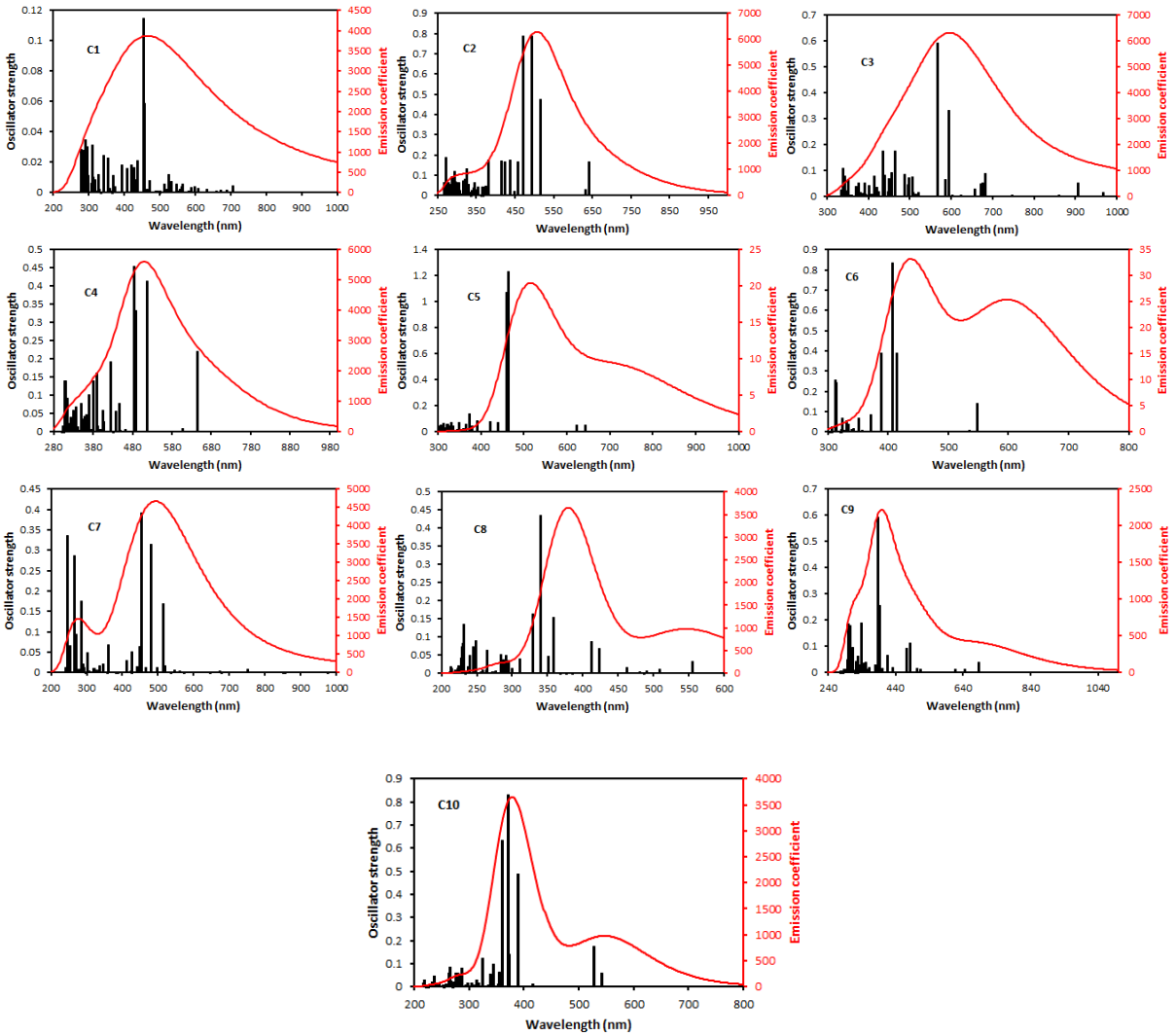

Figure 3: Computed electronic absorption (vertical bar) and emission (red line) spectra of the investigated corroles.

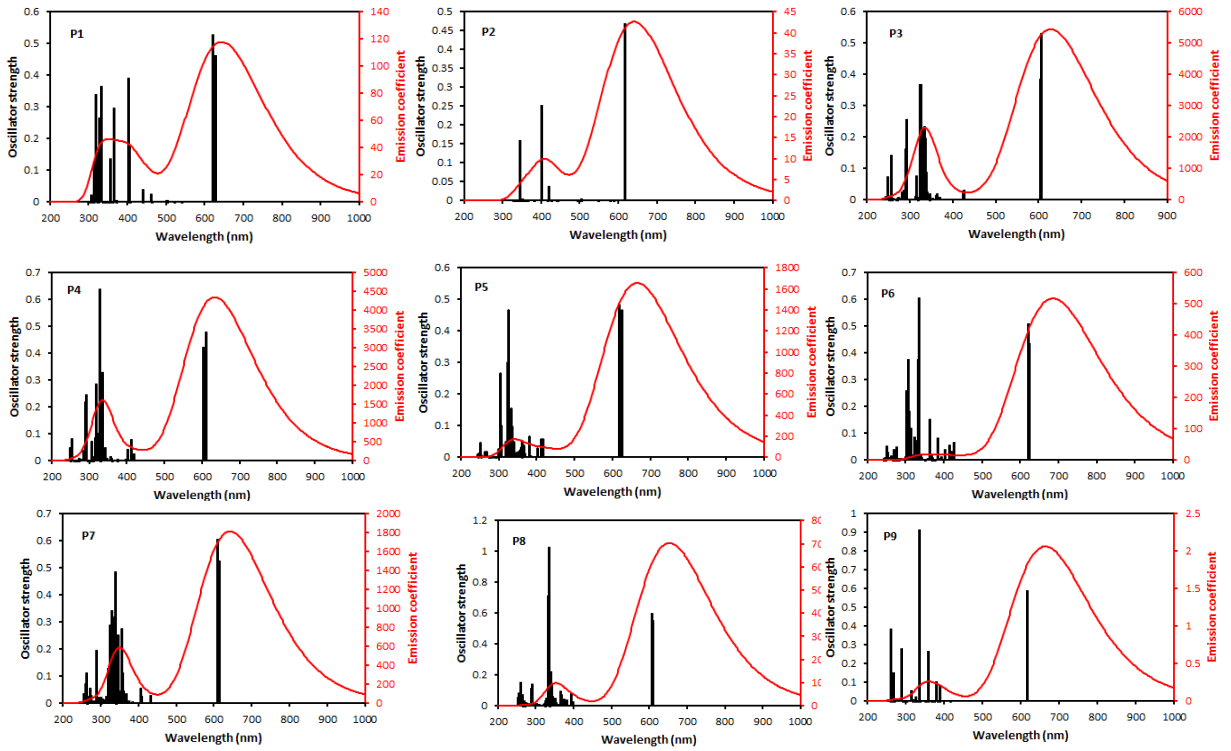

Figure 4: Computed electronic absorption (vertical bar) and emission (red line) spectra of the investigated phthalocyanines.

The energies of the dyes' highest occupied molecular orbital (HOMO) and lowest unoccupied molecular orbital (LUMO) are critical basis for evaluating their photostability and electron injection efficiency (ϕ_f) (Sanusi *et al*., 2019). The wider the HOMO-LUMO gap, the higher the energy of the incident photon required to excite electrons from the ground state (HOMO) to the excited LUMO state. Thus, a good dye sensitizer is expected to have an appreciably small HOMO-LUMO gap (Bourouina *et al*., 2017). The small energy gaps enhance electron excitation and lead to an increased photon absorption

(Mustafa *et al*., 2023), facilitating higher efficiency and a greater short-circuit current density.

Photophysicochemical and photovoltaic Properties

The photophysicochemical and photovoltaic properties of the studied dyes presented in Table 2 were determined following the literature procedure (Sanusi *et al*., 2019; Sanusi *et al*., 2023). Another factor that influences the photocurrent density in DSSCs and determines the rate of electron injection is the potential energy gap (δ_p) between the dye's LUMO and the conduction band (CB) edge of the semiconductor (Olguin *et al*., 2014). An efficient sensitizer must have its LUMO situated above the CB edge of the semiconductor. This would yield a positive δ_p value and signify that electron injection is thermodynamically favorable (*i.e*., a -ve ΔG_{inj} is obtained) (De Angelis *et al*., 2008). TiO_2 CB edge value obtained by experiment (-4.21 eV) was used to estimate δ_p values of the studied sensitizers (Xu and Schoonen, 2000). Except for compounds C1, C7, and P7 – P9, δ_p values were found to be positive for the studied corroles and Pcs (Table 2). The electron injection processes in these dyes are therefore expected to be spontaneous. Mn-based corroles (C1 and C7) were found to produce negative δ_p values, indicating that their LUMO is below the TiO_2 CB edge (Figure 6) and their electron injection would be thermodynamically unfavorable. The ideal δ_p value for efficient electron injection is ~0.40 eV (De Angelis *et al*., 2008). It is expected that the dyes' δ_p is at least ±0.5 near this recommended value to be suitable as sensitizers. The δ_p values obtained for the corroles and Pcs ranged between -12.4 – 7.10 eV and -5.71 – 7.92 eV, respectively (Table 2).

Compounds C1, C7 and P7 – P9 given by the negative values of their δ_p were predicted to show misalignment with the TiO_2 CB edge, implying that electron injection from their HOMO to the semiconductor CB edge would be thermodynamically unfavorable as revealed by their ΔG_{inj} values (Table 2).

They are the only set of the studied molecules with positive ΔG_{inj}. It should however be noted that those with positive δ_p showed significantly higher values than the optimum (0.4 eV), implying that the right amount of energy for efficient electron injection would not be available even though the transition from HOMO to the TiO_2 CB edge would be thermodynamically favored. The rate of the transition would be slow, resulting in an inefficient electron injection. The consequence of this would be a decrease in the photocurrent density. The metal-free corroles (C5 and C10) and Pcs (P1, P4, P6, and P7) were observed to possess smaller δ_p values relative to their metal-centered derivatives, which showed that the metal-free dyes have higher electron injection rate than their metal-centered analogues due to a possible spin-orbit coupling in the metal complexes (Sanusi *et al*., 2014). The Pc molecules with relatively smaller δ_p are P3, P4, P5 and P6. While P4 and P6 are metal-free Pcs, P3 and P5 have Zn as their central metal. It was observed that the other Pcs, P1, P2, P8 and P9, including a metal-free P7 have δ_p values that are unsuitable for DSSC application. Notably, these molecules are charged, and the charges appeared to be the common factor responsible for the extremely high or the negative δ_p values. The relative positions of the studied molecules with the TiO_2 CB edge have been depicted in Figures 5 and 6.

Table 2: Computed Photophysicochemical and Photovoltaic Properties of the Studied Corroles and Phthalocyanines

DYE	LUMO-HOMO Gap (eV)	δp (eV)	ΔG_{inj}	τ_f (ns)	Φ_f	LHE × 10^{-2}	η_c × 10^{-11}	*IPCE*
C1	1.18	-10.4	10.0	40.2	0.30	2.0	0.63	4.32×10^{-14}
C2	2.25	4.40	-4.08	39.8	0.08	16.0	3.49	4.54×10^{-13}
C3	1.05	6.80	-7.40	40.5	0.01	11.0	1.46	2.02×10^{-13}
C4	1.65	3.90	-4.16	40.2	0.10	12.0	4.47	5.42×10^{-13}
C5	2.36	1.70	-1.28	11.7	3.37×10^{-4}	14.0	23.6	1.14×10^{-14}
C6	2.56	4.10	-3.81	14.5	9.04×10^{-4}	10.0	3.92	3.76×10^{-15}
C7	0.55	-12.4	11.4	41.3	0.11	8.0	0.43	4.15×10^{-14}
C8	1.05	7.10	-7.59	40.3	0.83	7.0	1.33	8.27×10^{-13}
C9	2.83	3.90	-3.44	40.7	0.06	9.0	4.27	2.38×10^{-13}
C10	2.59	0.90	-0.58	40.1	0.05	12.0	87.5	5.29×10^{-12}
P1	2.08	7.80	-7.689	50.3	2.23×10^{-3}	11.9	1.17	3.09×10^{-15}
P2	2.16	7.92	-7.774	40.2	9.94×10^{-4}	6.80	1.10	7.41×10^{-16}
P3	2.14	1.48	-1.379	40.9	9.90×10^{-2}	13.2	33.17	4.32×10^{-12}
P4	2.13	1.45	-1.348	36.7	7.76×10^{-2}	14.0	35.75	3.90×10^{-12}
P5	2.11	1.81	-1.690	23.9	2.96×10^{-2}	12.5	20.49	7.57×10^{-13}
P6	2.08	1.75	-1.657	17.2	9.04×10^{-3}	13.4	22.44	2.72×10^{-13}
P7	2.13	-5.71	5.828	31.8	2.51×10^{-2}	17.5	1.95	8.55×10^{-14}
P8	2.16	-5.64	5.767	22.8	9.60×10^{-3}	17.0	1.96	3.20×10^{-14}
P9	2.13	-5.14	5.269	22.4	2.60×10^{-5}	19.6	2.63	1.35×10^{-16}

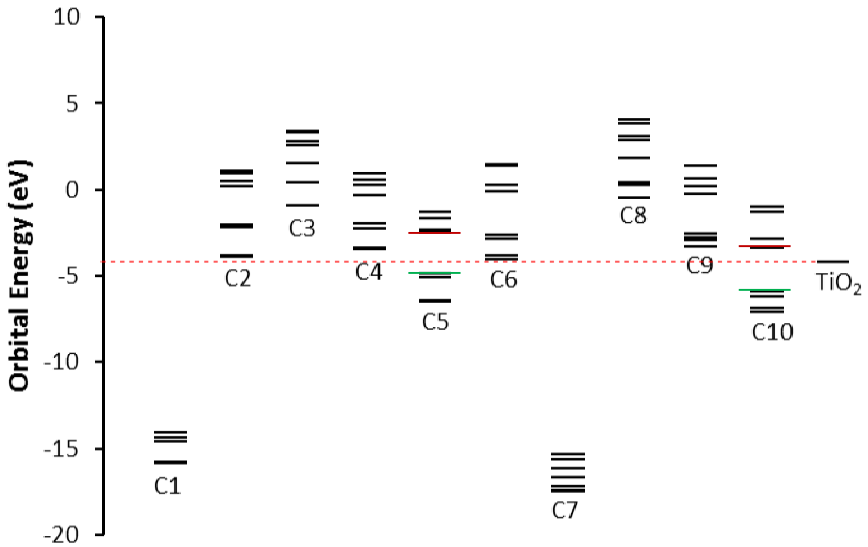

Figure 5: Computed orbital energy diagram of the corroles. The red and green lines at molecules C5 and C10 are the LUMO and HOMO levels, respectively. Other LUMOs and HOMOs were not indicated because their values have no relevant practical interpretation. The dashed red line indicates the relative positions of the molecules' LUMO to that of the TiO_2 CB edge.

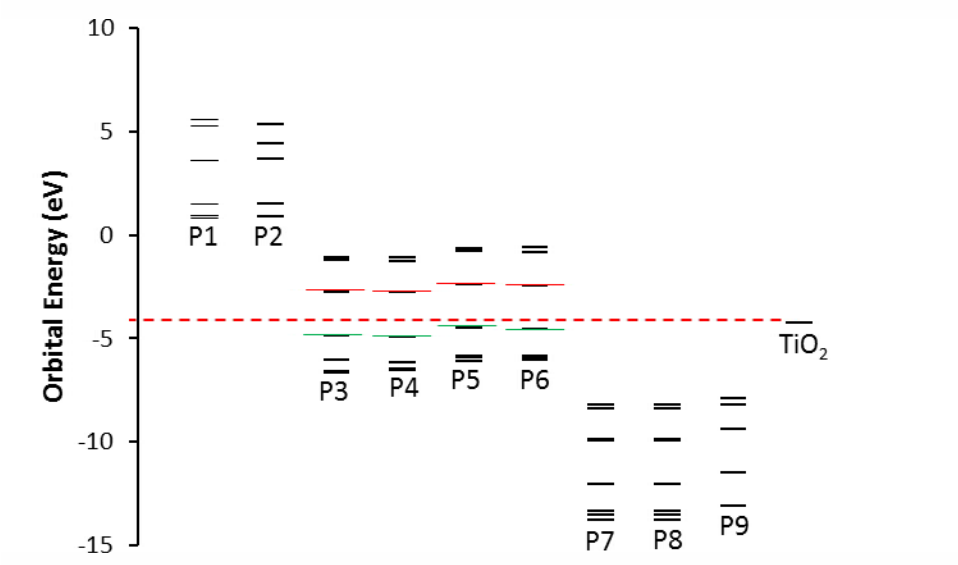

Figure 6: Computed orbital energy diagram of the phthalocyanines. The red and green lines at molecules P3 – P6 are the LUMO and HOMO levels, respectively. Other LUMOs and HOMOs were not indicated because their values have no relevant practical interpretation. The dashed red line indicates the relative positions of the molecules' LUMO to that of the TiO_2 CB edge.

The substituents and the metal centers in these molecules are evidently unsuitable to achieve the desired sensitization for solar cell application.

Light harvesting efficiency (*LHE*) measures the fraction of light intensity that is absorbed by the dye at a certain spectral range. The spectral range of interest in this study depends on the mean oscillator strength (*f*) obtained for the molecules at maximum absorption wavelength (λ_{max}) in the ultraviolet to the near IR region (Li *et al.*, 2010). Table 2 shows the estimated LHE values obtained for each of the studied molecules.

On the other hand, it was observed that metal-free phthalocyanine P1, P4, P6, and P7 which are derivatives of P2, P3, P5, and P8, respectively, have higher LHE values relative to their metal-centered counterparts (Table 2). This suggests that these dyes possess a greater capacity for absorbing light within the specified spectral range. This finding is in agreement with the conclusions drawn by Khan *et al.* (2020) that the presence of central metals can modify the geometry, conformation, packing density, and orientation of the dyes on the semiconductor surface. This in turn, influences the light harvesting efficiency the dyes. The same trend was observed for the corroles. The free and Zn-based corroles were found to have higher LHE values than the Fe-, Mn- and Cu-based corroles. This may be due to their better energy alignment with the TiO_2 conduction band than the other metallocorroles.

Compound P2 which is the only dye with Ni(II) has its central metal, displayed the lowest LHE value relative to all other dyes which are metal -free and Zn-based. This may be because Ni(II) has a lower oxidation potential than Zn(II) (Gara *et al*., 2023), thus making P2 less efficient in absorbing sunlight, donating electrons to the semiconductor, and forming a stable complex on the surface. Notably, molecule P9 had the highest LHE value, even though it has a metal center. It is worth noting that the general trend observed in the LHE values of the molecules suggest that positively charged dyes have better light absorbing property than a neutral dye which in turn are better than a negatively charged dye.

The charge collection efficiency (η_c) is the probability of electron availability at the TiO_2-dye interface. It is a ratio of the dye's diffusion coefficient by the square of the potential energy gap (δ_p) between the dye's LUMO and the TiO_2 CB edge (Sanusi *et al*., 2019). A high charge collection efficiency is required for a dye sensitizer to be considered effective. The η_c obtained for the molecules showed that C5, C10, P3, P4, P5, and P6 have the highest η_c values (Table 2). It has been established that metal-free dyes generally have a stronger electron-donating ability and a lower LUMO-CB edge gap than metallated dyes (Wang *et al*., 2019), meaning they can inject electrons into the TiO_2 conduction band more efficiently and reduce the recombination losses. This trend was observed for the phthalocyanines, where metal-free P1, P4, P6, and P7 have higher η_c values relative to their metallated analogues. Additionally, the η_c values of the corroles were found to decrease in the order metal-free corrole > Fe- > Zn- > Cu- > Mn- corroles, which was consistent with the order of decreasing δ_p. This suggests that the presence of metal atom affects the electron injection and recombination processes of the corrole sensitizers, thus affecting affects their PCE values.

The overall charge on the dye influences the adsorption strength and orientation of dye molecules on the TiO_2 surface through electrostatic interactions with the semiconductor (Bertoluzzi and Ma, 2013). It could be deduced that a neutral dye, with balanced electron density, would form a stable, uniform adsorption layer on TiO_2, which would aid electron injection and reduce recombination losses. In contrast, a positively charged dye, with high electron deficiency, would exhibit distorted electron density due to repulsion by the positively charged TiO_2 surface, causing a more tilted orientation that might inhibit electron injection and increase recombination losses. This same effect is also expected for a negatively charged sensitizer. Therefore, the dyes with overall neutral charge (C5, C10, P3, P4, P5, and P6) were found to show higher η_c relative to the positively charged dyes (C1, C7, P7, P8, and P9), which in turn showed higher η_c than the negatively charged dyes (C2, C3, C4, C6, C8, C9, P1, and P2), Table 2.

The IPCE describes the overall photovoltaic performance of a photosensitizer. They were obtained according to the method described previously by our group (Sanusi *et al*., 2019). It is interesting to note that out of all the molecules, only molecules C10, P3, and P4 produced the highest IPCE values (Table 2). These three molecules out of the ones

investigated, showed the best photovoltaic and photophysicochemical properties required for efficient solar cell applications. It should be noted however, that their performances still require significant improvement, which can be achieved by structural modification (Sanusi *et al*., 2023). Even though the dyes absorbed strongly in the required spectral range, their performances as photosensitizers were generally found to be poor, as most of the dyes, had low IPCE and high non-aligning δ_p values.

Conclusion

DFT methods were used to study the photovoltaic and photophysicochemical properties of some metal-free and metal-containing corroles (C1-C10) and phthalocyanines (P1-P9) for possible application as photosensitizers in DSSC. Time-dependent density functional theory (TD-DFT) methods were used to generate the electronic absorption spectra of the molecules. The absorption and emission energies of the studied dyes fall within the spectral range of 350 – 800 nm, as required for a good sensitizer. The δp values obtained for the corroles and Pcs are in the range of -12.4 – 7.10 eV and -5.71 – 7.92 eV, respectively, which are significantly larger than the ideal value of *ca* 0.40 eV. Compounds C5, C10, P3, P4, P5, and P6 showed a fairly situated energy levels for efficient electron injection and photocurrent generation. The metal-free dyes were found to have higher LHE and r_c values compared to their metallated analogues. Molecules C5, C10, P3, P4, P5, and P6 had the highest r_c values. In general, compounds C10, P3, and P4 with IPCE values in the order of 10^{-12} showed the best properties that are fairly suited for DSSC application. However, the photovoltaic performance of these set of molecules could be further improved through structural modification and extension of their π-conjugation.

Acknowledgements

The authors, in particular KS, NOF and PBK, are grateful to the management of the Centre for High Performance Computing (CHPC), South Africa, for giving us access to their central supercomputing cluster.

References

Ali, H. E. A., Altindal, A., Altun, S. and Odabaş, Z. (2016). Highly efficient dye-sensitized solar cells based on metal-free and copper(II) phthalocyanine bearing 2-phenylphenoxy moiety. *Dyes Pigment*, 124: 180 – 187.

Andrews, D. L., Cao, G. Z., and Gaburro, Z. (2004). *Nanophotonic Materials. SPIE*, 5510.

Aviv-Harel, I., and Gross, Z. (2009). Aura of corroles. *Chemistry A - European Journal*, 15(34), 8382-8394.

Aviv, I. and Gross, Z. (2007). Corrole-based applications. *Chemical Communications*, 20: 1987 – 1999.

Becke, A. D. (1992a). Density functional thermochemistry. I. The effect of the exchange only gradient correction. *Journal of Chemical Physics*, 96: 2155–2160.

Becke, A. D. (1992b). Density functional thermochemistry. II. The effect of the Perdew-Wang generalized gradient correlation correction. *Journal of Chemical Physics*, 97: 9173–9177.

Becke, A. D. (1993). Density functional thermochemistry. III. The role of exact exchange. *Journal of Chemical Physics*, 98: 5648–5652.

Bertoluzzi, L. and Ma, S. (2013). On the methods of calculation of the charge collection efficiency of dye sensitized solar cells. *Physical Chemistry Chemical Physics*, 15(12): 4283-4285.

Bourouina, A., Rekhis, M., and Trari, M. (2017). DFT/TD-DFT study of ruthenium bipyridyl-based dyes with a chalcogen donor (X= S, Se, Te), for application as dye-sensitized solar cells. *Polyhedron*, 127, 217-224.

Brennan, B. J., Lam, Y. C., Kim, P. M., Zhang, X. and Brudvig, G. W. (2015). Photoelectrochemical cells utilizing tunable corroles. *ACS Applied Material Interfaces*, 7(29): 16124 – 16130.

Carella, A., Borbone, F. and Centore, R. (2018). Research progress on photosensitizers for DSSC. *Frontiers in Chemistry*, 6: 481–505.

De Angelis, F., Fantacci, S. and Selloni, A. (2008). Alignment of the dye's molecular levels with the TiO_2 band edges in dye-sensitized solar cells: A DFT–TD-DFT study. *Nanotechnol*ogy, 19: 424002 – 424010.

Frank, A. J., Kopidakis, N., De Lagemaat, J. V. (2004). Electrons in nanostructured TiO_2 solar cells: Transport, recombination and photovoltaic properties. *Coordination Chemistry Review* 248: 1165–1179.

Gara, R., Zouaghi, M. O. and Arfaoui, Y. (2023). Porphyrin and phthalocyanine heavy metal removal: overview of theoretical investigation for heterojunction organic solar cell applications. *Journal of Molecular Modeling*,, 29(8), 259.

Gaussian 16, Revision C.01, Frisch, M. J., Trucks G. W., Schlegel, H. B., Scuseria, G. E, Robb, M. A., Cheeseman, J. R., Scalmani, G., Barone, V., Petersson, G. A, Nakatsuji, H., Li, X., Caricato M, Marenich AV, Bloino J, Janesko BG, Gomperts R, Mennucci B, Hratchian HP, Ortiz, J. V, Izmaylov, A. F., Sonnenberg, J. L., Williams-Young, D., Ding, F., Lipparini, F., Egidi, F., Goings, J., Peng, B., Petrone, A., Henderson, T., Ranasinghe, D., Zakrzewski, V. G., Gao, J., Rega, N., Zheng, G., Liang, W., Hada, M., Ehara, M., Toyota, K., Fukuda, R., Hasegawa, J., Ishida, M., Nakajima, T., Honda, Y., Kitao, O., Nakai, H., Vreven, T., Throssell, K., Montgomery, J. A. Jr, Peralta, J. E., Ogliaro, F., Bearpark, M. J., Heyd, J. J., Brothers, E. N., Kudin, K. N., Staroverov, V. N., Keith, T. A., Kobayashi, R., Normand, J., Raghavachari, K., Rendell, A. P., Burant, J. C., Iyengar, S. S., Tomasi, J., Cossi, M., Millam, J. M., Klene, M., Adamo, C., Cammi, R., Ochterski, J. W., Martin, R. L., Morokuma, K., Farkas, O., Foresman, J. B., Fox, D. J. (2019) Gaussian, Inc., Wallingford CT.

Gorduk, S. (2019). Synthesis, photophysics and photochemistry studies on nonperipherally

tetra-substituted Zn(II) and In(III) phthalocyanines bearing ferulic acid units. *Journal of Molecular Structure,* 1198: 126921-126940.

Gorduk, S. and Altindal, A. (2019). Peripherally tetra-substituted metallophthalocyanines bearing carboxylic acid groups for efficient dye sensitized solar cells. *Journal of Molocular Structure,* 1196: 747–753.

Hamann, T. W., Jensen, R. A., Martinson, A. B., Van Ryswyk, H. and Hupp, J. T. (2008). Advancing beyond current generation dye-sensitized solar cells. *Energy and Environmental Science,* 1(1): 66–78.

Higashino, T., Kurumisawa, Y., Alemayehu, A. B., Einrem, R. F., Sahu, D., Packwood, D.
- and Imahori, H. (2020). Heavy Metal Effects on the Photovoltaic Properties of Metallocorroles in Dye-Sensitized Solar Cells. *ACS Applied Energy Material,* 3(12): 12460-12467.

nternational Energy Agency. (n.d.). 2017. *World energy outlook 2020.* Retrieved from https://www.iea.org/reports/world-energy-outlook-2020.

Karaca, H., Şişman, Ì., Güzel, E., Sezer, S., Selimoğlu, F., Ergezen, B., Karaca, M. and Eyüpoğlu, V. (2018). Thiochalcone substituted phthalocyanines for dye-sensitized solar cells: Relation of optical and electrochemical properties for cell performance. *J. Coordination Chemistry*, 71(10): 1606 – 1622.

Khan, M. S., Khalid, M., and Shahid, M. (2020). What triggers dye adsorption by metal Organic frameworks? The current perspectives. *Materials Advances,* 1(6): 1575-1601.

Lakowicz, J. R. (2006). Principles of fluorescence spectroscopy (2nd ed.). Springer Science & Business Media. Kluwer Academic/ Plenum Publishers, New York, 1999239.

Lee, C., Yang, W., Parr, R. G. (1988). Development of the Colle-Salvetti correlation-energy formula into a functional of the electron density. *Physical Review B* 37: 785–789.

Li, C., Liu, M., Pschirer, N. G., Baumgarten, M., and Müllen, K. (2010). Polyphenylene-Based Materials for Organic Photovoltaics. *Chemical Review,* 110, 6817–6855.

Mathew, S., Yella, A., Gao, P., Humphry-Baker, R., Curchod, B. F. E., Ashari-Astani, N., Tavernelli, I., Rothlisberger, U., Nazeeruddin, M. K. and Grätzel, M. (2014). Dye-sensitized solar cells with 13% efficiency achieved through the molecular engineering of porphyrin sensitizers. *Nature Chemistry,* 6(3): 242–247.

Mustafa, F. M., Abdel Khalek, A. A., Mahboob, A. A., and Abdel-Latif, M. K. (2023). Designing Efficient Metal-Free Dye-Sensitized Solar Cells: A Detailed Computational Study. *Molecules,* 28(17): 6177-6194.

Noomnarm, U. and Clegg, R. M. (2009). Fluorescence lifetimes: Fundamentals and interpretations, *Photosynthesis Research,* 101(2-3): 181-194.

Olguin, M., Basurto, L., Zope, R. R. and Baruah, T. (2014). The effect of structural changes

on charge transfer states in a light-harvesting carotenoid-diaryl-porphyrin-C60 molecular triad. *Journal of Chemical Phys*ics, 140: 204309 – 204326.

Pierloot K., Zhao H., and Vancoillie S. (2010). Copper corroles: the question of noninnocence. *Inorganic Chemistry*, 49: 10316–10329.

Polat, M. P., Yenilmez, H. Y., Koca, A., Altindal, A. and Bayir, Z. A. (2018). Metallophthalocyanines bearing four 3-(pyrrol-1-yl)phenoxy units as photosensitizer for dye-sensitized solar cells. *Dyes Pigments*, 156: 267 – 275.

Pomarico, G., Nardis, S., Paolesse, R., Ongayi, O. C., Courtney, B. H., Fronczek, F. R., & Vicente, M. G. H. (2011). Synthetic routes to 5, 10, 15-triaryl-tetrabenzocorroles. *Journal of Organic Chemistry*, 76(10): 3765-3773.

Pomarico, G., Nardis, S., Stefanelli, M., Cicero, D. O., Vicente, M. G. H., Fang, Y., Chen, P., Kadish, K. M., & Paolesse, R. (2013). Synthesis and characterization of functionalized *meso*-triaryltetrabenzocorroles. *Inorganc Chemistry*, 52(15): 8834-8844.

Raffaelle, R. (2006). 'Hybrid nanomaterials improve solar cell efficiency.' *SPIE Newsroom*.

Sanusi, K., Antunes, E. and Nyokong, T. (2014). Optical nonlinearities in non-peripherally substituted pyridyloxy phthalocyanines: a combined effect of symmetry, ring-strain and demetallation. *Dalton Transactions*, 43: 999 – 1010.

Sanusi, K., Atewolara-Odule, O. C., Sanyaolu, N. O., Ibikunle, A. A., Khoza, P. B., Fatomi, N. O., Fasanya, S. A., Abuka, H. E., Jesugbile, E. O., Yilmaz, Y., Ceylan, Ü. (2023). Effects of solvents and substituents on the adsorptive and photovoltaic properties of porphyrins for dye-sensitized solar cell application: A theoretical consideration. *Structural Chemistry*, 34:891–904.

Sanusi, K., Ceylan, Ü., Yilmaz, Y. and George, R. C. (2020). A DFT/TDFT study on the possible replacement of Ru(II) with Fe(II) in phthalocyanine-based dye-sensitized solar cells. *Structural Chemistry*, 31: 2301 – 2311.

Sanusi, K., Fatomi, N. O., Aderogba, A. A., Khoza, P. B., and Igumbor, E. (2023). A DFT Study of Solvent and Substituent Effects on the Adsorptive and Photovoltaic Properties of Some Selected Porphyrin Derivatives for DSSC Application. *Journal of Fluorescence*, 1-10.

Sanusi, K., Fatomi, N. O., Borisade, A. O., Yilmaz, Y., Ceylan, Ü., Fashina, A. (2019). An approximate procedure for profiling dye molecules with potentials as sensitizers in solar cell application: A DFT/TD-DFT approach. *Chem*ical *Phys*ics *Letters*, 723: 111–117.

Snaith, H. J. (2010). Estimating the Maximum Attainable Efficiency in Dye-Sensitized Solar Cells. *Advanced Functional Materials*, 20: 13–19.

Srikanth, M., Sastry, G. N. and Soujanya, Y. (2015). Molecular design of corrole-based D-π-A sensitizers for dye-sensitized solar cell applications. *International Journal of Quantum Chemistry*, 115(12): 745 – 752.

Sudhakar, K., Giribabu, L., Salvatori, P., & Angelis, F. D. (2015). Triphenylamine7 functionalized corrole sensitizers for solar‐cell applications. *physica status solidi (a)*, 212(1): 194-202.

The World Bank. (n.d.). *Access to Electricity (% of population) [Data file]*. World Development Indicators. Retrieved November 12, 2021, from https://data.worldbank.org/indicator/EG.ELC.ACCS.ZS

Tunç, G., Güzel, E., Şişman, Ì., Ahsen, V., Cárdenas-Jirón, G. and Gürek A. G. (2019). Effect of new asymmetrical Zn(II) phthalocyanines on the photovoltaic performance of a dye-sensitized solar cell. *New Journal of Chem*istry, 43: 14390 – 14401.

Urbani, M., Ragoussi, M.-E., Nazeeruddin, M. K. and Torres, T. (2019). Phthalocyanines for dye-sensitized solar cells. Coordination *Chemistry Review*, 381: 1–64.

Wang, G., Deng, J., Wang, X., Liu, J., Chen, Y., & Liu, B. (2019). An electron donating controlling strategy for design several dithieno [3, 2-b: 2′, 3′-d] pyrrole-based dyes with D–D–A structure in dye-sensitized solar cells. *Journal of Materials Science: Materials in Electronics*, 30: 20525-20536.

Xu, Y. and Schoonen, M. (2000). The absolute energy positions of conduction and valence bands of selected semiconducting minerals. *American Mineralogist*, 85: 543-556.

Zhu, C. and Liang, J-X. (2015). Theoretical insight into novel zinc di-corrole de with excellent photoelectronic properties for solar cells. *New Journal of Chem*istry, 39, 3624 – 3628.